The Astrophysical Journal, 547:L123–L127, 2001 February 1

TIDAL STIRRING AND THE ORIGIN OF DWARF SPHEROIDALS IN THE LOCAL GROUP

Lucio Mayer,[1,2] Fabio Governato,[3] Monica Colpi,[1] Ben Moore,[4] Thomas Quinn,[2]
James Wadsley,[2,5] Joachim Stadel,[2] and George Lake[2]
Received 2000 June 27; accepted 2000 November 9; published 2001 January 23

ABSTRACT

N-body + smoothed particle hydrodynamics (SPH) simulations are used to study the evolution of dwarf irregular galaxies (dIrr's) entering the dark matter halo of the Milky Way or M31 on plunging orbits. We propose a new dynamical mechanism driving the evolution of gas-rich, rotationally supported dIrr's, mostly found at the outskirts of the Local Group (LG), into gas-free, pressure-supported dwarf spheroidals (dSph's) or dwarf ellipticals (dE's), observed to cluster around the two giant spirals. The initial model galaxies are exponential disks embedded in massive dark matter halos and reproduce nearby dIrr's. Repeated tidal shocks at the pericenters of their orbits partially strip their halos and disks and trigger dynamical instabilities that dramatically reshape their stellar components. After only 2–3 orbits low surface brightness dIrr's are transformed into dSp'hs while high surface brightness dIrr's evolve into dE's. This evolutionary mechanism naturally leads to the morphology-density relation observed for LG dwarfs. Dwarfs surrounded by very dense dark matter halos, such as the dIrr GR8, are turned into Draco or Ursa Minor, the faintest and most dark matter dominated among LG dSph's. If disks include a gaseous component, this is both tidally stripped and consumed in periodic bursts of star formation. The resulting star formation histories are in good qualitative agreement with those derived using *Hubble Space Telescope* (*HST*) color-magnitude diagrams for local dSph's.

Subject headings: galaxies: dwarf — galaxies: evolution — galaxies: interactions — galaxies: kinematics and dynamics — Local Group — methods: *n*-body simulations

1. INTRODUCTION

Dwarf galaxies in the Local Group (LG) clearly obey a morphology-density relation. Close to the Milky Way and M31 we find early-type dwarf galaxies, namely, faint ($M_B > -14$) low surface brightness dwarf spheroidals (dSph's) and more luminous ($M_B > -17$), higher surface brightness dwarf ellipticals (dE's). All these galaxies are nearly devoid of gas, contain dark matter and mainly old stars, and are supported by velocity dispersion (Ferguson & Binggeli 1994, hereafter FB94; Mateo 1998, hereafter Ma98; Grebel 1999, hereafter Gr99; van den Bergh 1999). Among them Draco and Ursa Minor have the highest dark matter densities ever measured (Lake 1990). On the outskirts of the LG we find similarly faint ($M_B > -18$) and dark matter–dominated dwarf irregular galaxies (dIrr's) that are gas-rich, star-forming systems with disklike kinematics (Ma98; van den Bergh 1999; Gr99).

Previous attempts to explain the origin of dSph's in the LG have relied on gasdynamical processes to remove the gas in dIrr's. Gas stripping may result either because of the pressure exerted by an external hot gaseous medium in the halo of the Milky Way ("ram pressure"; Einasto et al. 1974) or because of internal strong supernova winds (Dekel & Silk 1986). However, ram pressure would require an external gas density that is several orders of magnitude higher than recently inferred for the Milky Way (Murali 2000) and supernova winds cannot explain the existing morphology-density relation. Moreover, such dissipative mechanisms would remove the gas but would not directly alter the structure and kinematics of the preexisting stellar component. However, the light follows an exponential profile in both dSph's and dIrr's (Faber & Lin 1983; Irwin & Hatzdimitriou 1995; Ma98) and a positive correlation between surface brightness and luminosity is shown by both types of dwarfs (FB94), suggesting an evolutionary link between them. Is there a mechanism that can transform dwarf galaxies between morphological classes, or must we accept the idea that dSph's are fundamentally different from dIrr's?

Within rich galaxy clusters, fast flyby encounters with the largest galaxies can transform a disk system into a spheroidal or S0 galaxy in just 3–4 Gyr (Moore et al. 1996; Moore, Lake, & Katz 1998). If the halos of bright galaxies were scaled-down versions of galaxy clusters, then this "galaxy harassment" would be equally important within them. However, whereas rich clusters contain over 30 large (L_*) perturbing galaxies, the Milky Way and M31 have only a couple of satellites sufficiently massive to harass the other dwarf galaxies (Moore et al. 1999; Klypin et al. 1999). As a result, the rate for effective satellite-satellite flyby encounters is less than one in every 10 Gyr (the LMC and the SMC being a notable exception).

Thus, we are left with only the repeated action of tidal forces from the primary galaxy as an evolutionary driver. These operate on the orbital timescale, which is of order of 3–4 Gyr in both clusters and galactic halos. However, given the relatively low age of large, virialized clusters, galaxies have typically approached the cluster center only once by the present time, while dSphs' satellites have had sufficient time to complete several close tidal encounters with the Milky Way, as stellar ages imply that the latter was already in place 10 Gyr ago (van den Bergh 1996).

In this Letter we use very high resolution *N*-body + smoothed particle hydrodynamics (SPH) simulations performed with the parallel binary tree code GASOLINE (Di-

[1] Dipartimento di Fisica, Università Degli Studi di Milano-Bicocca, via Celoria 16, I-20133 Milano, Italy; lucio.mayer@uni.mi.astro.it; monica.colpi@uni.mi.astro.it.
[2] Osservatorio Astronomico di Brera, via Bianchi 46, I-23807 Merate (LC), Italy; fabio@merate.mi.astro.it.
[3] Department of Astronomy, University of Durham, Durham, UK, DH1 3LE; ben.moore@durham.ac.uk.
[4] Department of Astronomy, University of Washington, Seattle, WA 98196; trq@astro.washington.edu; stadel@astro.washington.edu; lake@astro.washington.edu.
[5] Department of Physics and Astronomy, McMaster University, Hamilton, Ontario L8S 4M1, Canada; wadsley@physics.mcmaster.ca.

kaiakos & Stadel 1996; J. Wadsley, T. Quinn, & J. Stadel 2001, in preparation) to follow the evolution of small galaxies resembling dIrr's as they move on bound orbits in the tidal field of the massive dark matter halo of the Milky Way.

2. MODELS OF DWARF GALAXIES

The Milky Way halo is modeled as the fixed potential of a truncated isothermal sphere with a total mass $4 \times 10^{12}\ M_\odot$ inside a radius of 400 kpc, consistent with both recent measures based on radial velocities of distant satellites (Wilkinson & Evans 1999) and with generic models of structure formation (Peebles et al. 1989). The core radius is 4 kpc, and the resulting circular velocity at the solar radius is 220 km s^{-1}. Our simulated galaxies are modeled as exponential disks of stars with a Toomre parameter $Q = 2$ embedded in truncated isothermal dark matter halos (see Hernquist 1993). The number of particles in the disk is 50,000, while that in the halo ranges from 250,000 to 3×10^6. Such high resolution in the halo reduces considerably numerical heating of the disk due to massive halo particles, as was tested by evolving our models in isolation for 5 Gyr. The scale lengths and masses of the stellar disk and dark matter halo are chosen so that the satellites follow the observed *B*-band Tully-Fisher relation (Hoffman et al. 1996; Zwaan et al. 1995) and have realistic rotation curves (de Blok & McGaugh 1997; Cote, Freeman, & Carignan 1997), as shown in Figure 1.

The determination of general scaling properties of galaxies becomes more uncertain at the very faint end. Current structure formation models predict that the mass M and scale radius R of halos (and of their embedded disks) vary with redshift as $\sim(1 + z)^{-3/2}$ for a fixed value of the circular velocity V_c, with $V_c \sim R \sim M^{1/3}$ (Mo, Mao, & White 1998). The scaling with redshift reflects the fact that low-mass halos form at early epochs and have higher characteristic densities because the average density of the universe was higher. Galaxies with total masses less than $10^9\ M_\odot$ should typically form at $z \geq 2$ (Lacey & Cole 1993) and should live in halos with a central dark matter density $\sim 0.3\ M_\odot\ \mathrm{pc}^{-3}$, comparable to that inferred for GR8, an extremely faint LG dIrr (Carignan, Beaulieu, & Freeman 1990). The model with the smallest mass ("GR8") was built following these prescriptions.

The models cover the entire luminosity function of irregulars in the LG (Ma98) with stellar masses of 1.2×10^6 ($M_B = -11.2$, "GR8"), 9×10^8 ($M_B = -16.23$, "M2"), and $2.5 \times 10^9\ M_\odot$ ($M_B = -18$, "M1"). At fixed disk mass (either M1 or M2) we also vary the disk scale length, obtaining high surface brightness (HSB) satellites ($\mu_B = 21.5$ mag arcsec^{-2}, M1H and M2H) or low surface brightness (LSB) $\mu_B = 24.5$ or $M_B = -11.223.5$ mag arcsec^{-2}, M1La, M2La, M2Lb) for a total of six different models (we always assume $M/L_B = 2$ for the stellar disk and set the halo core radius equal to the disk scale length; see de Blok & McGaugh 1997). The GR8 model was obtained by rescaling model M1La for $z = 2$. The disk scale length r_h is only 76 pc for GR8, while those of the other models are, respectively, 1.3 or 2 kpc (HSB satellites) and 1.5, 3.2, or 4.8 kpc (LSB satellites). The total mass-to-light ratios at $3r_h$ (close to the peak of the rotation curves) are, respectively, 6 (HSB satellites), 12 (LSB satellites), and 32 (GR8).

3. EVOLUTION OF DWARF GALAXIES

As the Milky Way halo is modeled as an external potential, dynamical friction is neglected, which is a good approximation for satellites ~100 times less massive than the primary halo

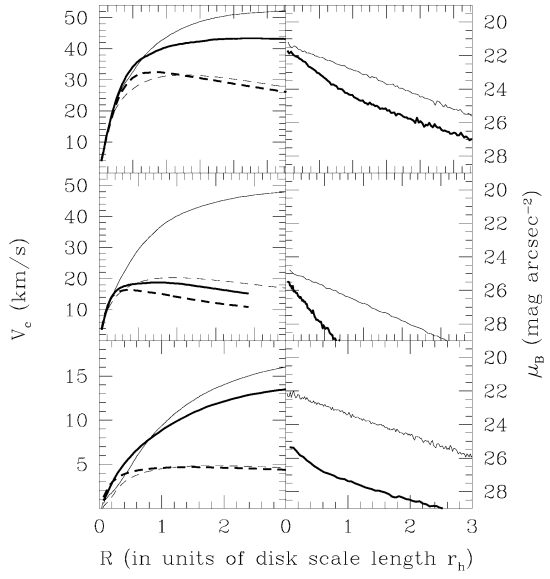

FIG. 1.—Evolution of (*left*) circular velocity and (*right*) surface brightness profiles for our model galaxies: thin lines are used for the initial profiles, thick lines for the profiles after 7 Gyr (the dashed line represents the contribution of the stars only). *Top to bottom:* Models M2H, M2La, and GR8, all placed on orbits with apo/peri = 9. For the final surface brightness profile we take into account fading according to the star formation histories described in the text (for GR8 we assume the history of the LSB with an earlier infall time).

(Colpi, Mayer, & Governato 1999). Satellites start at the virial radius of the primary (their apocenter) as if they were infalling for the first time, moving on orbits whose ratio between apocenter and pericenter ranges from 4 to 10, in agreement with simulations of galaxy and cluster formation (Ghigna et al. 1998). Orbital periods are typically of the order of 3–4 Gyr but are as short as 1–2 Gyr in the run with GR8 because this model was evolved in a Milky Way potential scaled down in size and mass as expected at $z = 2$. The inclination and spin of the disk relative to the orbital plane are randomly selected. In total 40 different runs were performed.

3.1. *Dynamical Evolution*

As the dwarfs approach pericenter (typically of 40–70 kpc) LSB satellites lose most of their dark and stellar mass, because of their low-density halos and large disks, and become weakly bar unstable. HSB satellites suffer modest stripping, and their more
self-gravitating disks develop strong bars. The GR8 model is barely stripped owing to its very dense halo and its small disk radius. Minimal stripping keeps its disk more self-gravitating compared with the structurally similar LSB satellites, and thus a fairly strong bar can develop after the second pericenter passage. Mass stripping for the various models is reflected in the evolution of their circular velocity profiles (Fig. 1). After completion of 2–3 orbits in 7 Gyr, our "tidally stirred" dwarf galaxies bear a striking resemblance to the real dSph's (*right panel* in Fig. 2): direct tidal heating coupled with the buckling of the bar due to bending instabilities (Raha et al. 1991) transmute the small disks into spheroids supported by velocity dispersion instead of rotation (Fig. 3). The GR8-like dwarf, falling into the Milky Way halo around redshift 2, suffers several (five) strong tidal shocks by the present time and is thus transformed despite being extremely compact.

On average the final v/σ (i.e., the ratio of the rotational to

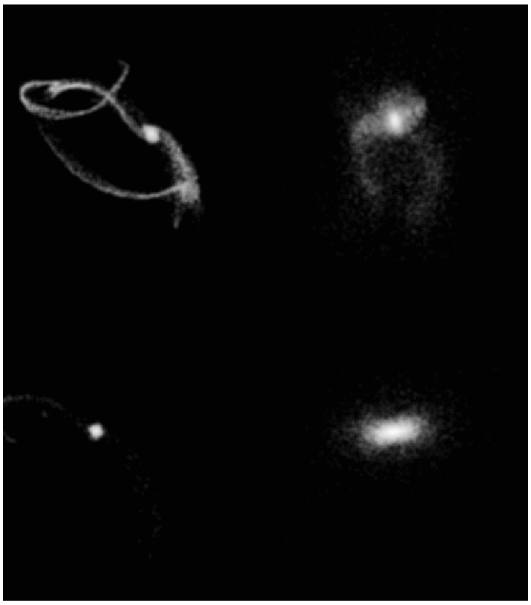

FIG. 2.—Final stellar configurations of the model galaxies. *Left:* Stellar streams of the (*top*) LSB and (*bottom*) HSB satellites viewed face-on (the orbit has apo/peri = 4). The boxes are 500 kpc on a side, with brighter colors showing regions with higher density. *Right:* Close-up views of the remnants seen edge-on in frames of 50 kpc on a side.

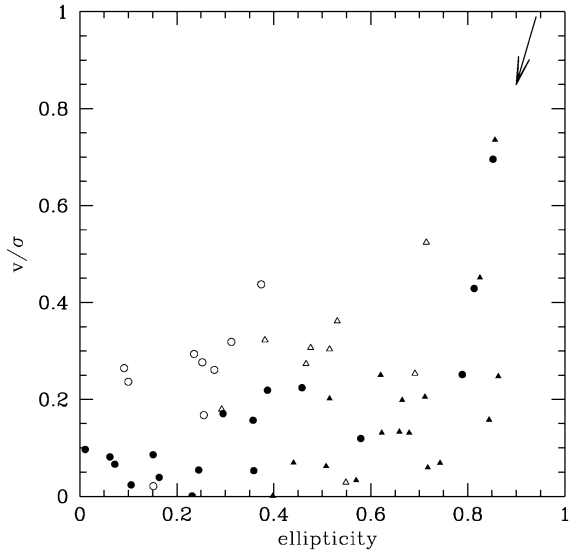

FIG. 3.—Final v/σ normalized to the initial value vs. final ellipticity for 26 different runs (measures are inside R_e). For each final state we show results for a line of sight aligned with the major axis of the remnant (*circles*) and with the intermediate axis (*triangles*). Filled symbols are for LSB satellites, open symbols for HSB satellites. The arrow indicates the initial states and shows the direction of evolution. The ellipticity is either $1 - c/b$ or $1 - c/a$ (with a, b, and c being, respectively, the major, intermediate, and minor axes of the remnants).

random velocity) inside the half-mass radius R_e drops to a mean value ≤ 0.5 (Fig. 3) and σ varies in the range 7–35 km s^{-1}, as observed for dSph's and dE's in the LG (Ma98). The largest of these values are typical of HSB remnants and are comparable to the velocity dispersion measured for the dE's associated with M31 (Ma98). Only when the satellite is initially in retrograde rotation with respect to its orbital motion do we measure a final v/σ still close to 1. The surface brightness profiles remain close to exponential (Fig. 1), although with a smaller scale length (typically by a factor of ~2). The remnants of HSB satellitess exhibit a steeper profile inside R_e because stars more efficiently lose angular momentum because of the strong bar instability. From this set of more than 40 runs a clear trend emerges: *LSB satellites evolve into objects resembling dSph's, while HSB satellites transmute into dE's*.

3.2. *Gasdynamics and Star Formation History*

Dwarf irregular galaxies have in general total H I–to–stellar mass ratios larger than 1 (Hoffman et al. 1996), but within the optical radius ($\sim 3r_h$) the neutral hydrogen fraction often drops to less than 50% of the stellar mass (Jobin & Carignan 1990; Cote et al. 1997). In some of our model galaxies we include a gaseous disk of 20,000 particles with a mass ~40% of the stellar disk mass (the gas density drops to zero at a radius $R < 0.5r_h$ to mimic the "holes" found in many dIrr's). The dynamics of gas are implemented using an SPH scheme and radiative cooling for a primordial mixture of hydrogen and helium (J. Wadsley et al. 2001). The initial temperature of the gas is set at 5000 K.

We place an LSB satellite (model M2La) on a 9 : 1 orbit: more than 50% of the gas is stripped after two pericenter passages and is never reaccreted, while the rest is torqued by the weak bar and gradually flows to the center: the surface density profile of the gas bound to the system steepens remarkably at each pericenter passage because of tidal compression and torques.

We then use Kennicutt's law (Kennicutt 1998) to determine the star formation rate from the gas surface density. We also take into account the reduction of the gas mass as it is converted into stars. The resulting star formation history has two main peaks roughly separated by the orbital time of the dwarf (~3.5 Gyr; Fig. 4), as recently found for Leo I and Carina (Hernandez, Gilmore, & Valls-Gabaud 2000). After 10 Gyr the star formation is suppressed because of gas consumption.

The stronger bar instability in an HSB satellite (model M2H) placed on the same orbit funnels more than 80% of the gas to the center at the first pericentric passage, giving rise to a starburst 10 times stronger than the bursts in the LSB satellites and using up all the gas in ~2 Gyr. As the strength of the bar instability seems to determine the type of star formation history, including gas in the GR8 model would lead to a result qualitatively similar to that of the HSB satellites. Interestingly, in the LG both the dE's and the extreme dSph's such as Draco and Ursa Minor formed the bulk of their stellar population during a single early episode (Ma98; Gr99).

Finally, we convolve the star formation history with the passive luminosity evolution of the stellar component resulting from population synthesis models (Bruzual & Charlot 1993) for low-metallicity systems ($\frac{1}{4}$ of the solar value). The multiple bursts are modeled as decreasing exponential laws with amplitude and time constants constrained by the numerical results. The resulting total B-band luminosities and stellar mass-to-light ratios of the final remnants are in good agreement with those of observed dSph's.

4. DISCUSSION

Figure 5 summarizes the main observable properties of the simulated satellites, projecting them on the fundamental plane (FB94). The remnants of LSB satellites resemble dSph's such as Fornax or Sagittarius ($-14 < M_B < -11$), while HSB satellites transform into the bright dE's ($M_B > -17$), having final

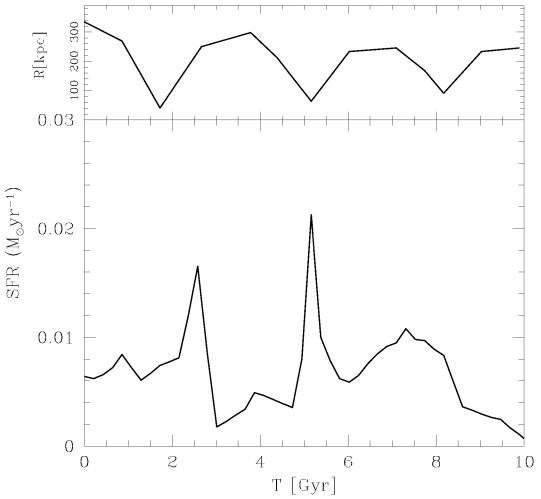

FIG. 4.—Star formation history for an LSB dwarf. The dwarf enters the Milky Way halo at $t = 0$. The orbital evolution is shown on top.

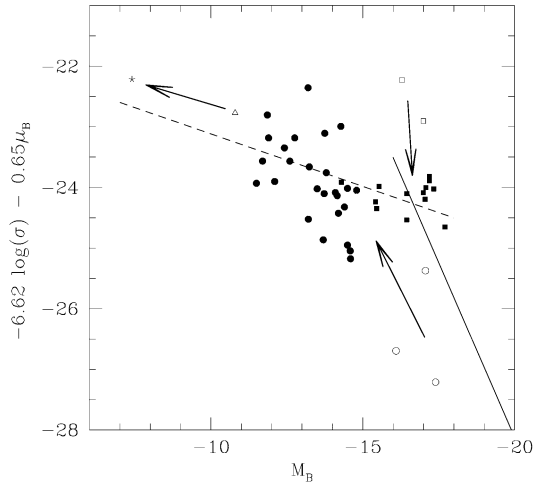

FIG. 5.—Fundamental plane (FP) for all the remnants as in FB94. In the FP plot, μ_B and σ are the average surface brightness and velocity dispersion measured inside R_e, and M_B is measured at the Holmberg radius. The dashed line is a fit to the distribution of local dSph's, while the solid line refers to elliptical galaxies within the Virgo cluster. Open and filled symbols represent, respectively, the initial and final states of HSB satellites (*squares*) and LSB satellites (*circles*). The initial and final states of the GR8 model are indicated by the open triangle and asterisk.

central surface brightnesses higher than those of observed dIrr's with the same luminosities and therefore matching another observational constraint (FB94; Ma98). The total (including dark matter) final mass-to-light ratios are in the range 6–20. Remarkably, our model can reproduce the properties of even the most extreme dSph's, Draco and Ursa Minor. In fact, as the dark matter halo of GR8 is barely affected by tides (Fig. 1), the remnant ($M_B = -7.5$) has a final mass-to-light ratio still ~50 and the central dark matter density is still around 0.3 $M_\odot$ pc^{-3}, matching the structural parameters inferred for Draco and Ursa Minor (Ma98).

"Tidal stirring" naturally leads to the spatial segregation of dIrr's versus dSph's, as its effectiveness depends strongly on the distance from the primary.

How important is our assumption of a massive and extended dark matter halo surrounding the Milky Way? When we adopt a "minimal" dark halo truncated at 50 kpc (with mass $5 \times 10^{11}\ M_\odot$; Little & Tremaine 1987), tides are too weak and the final remnants are still rotationally flattened ($v/\sigma > 1$). Instead, within a halo as massive and extended as implied by theories of galaxy formation (Peebles 1989), our dIrr models transform into dSph's even on orbits with apocenters larger than 200 kpc, explaining the origin of even the farthest dSph's such as Leo I and Leo II.

Though rather speculative at this stage, it is tempting to relate HSB satellites observed during the strong bursting phase to the population of blue compact dwarfs identified by Guzmán et al. (1997) at intermediate redshift. Redshift surveys will establish whether bursting dwarfs have nearby massive companions.

Extended tidal streams of stars originate from our simulated dwarfs (Fig. 2) with a maximum surface brightness of just 30 mag arcsec^{-2} (B band). Spectroscopic evidence for stellar streams from the dSph Carina has been recently claimed (Majewski et al. 2000).

Our model successfully explains the origin of dSph's once all observational constraints are taken into account: they evolved from dIrr's that entered the halo of the Milky Way or M31 several billion years ago moving on plunging orbits and suffered stirring by the tidal field of the large spirals.

The authors thank G. Bothun for stimulating discussions. Simulations were carried out at the CINECA (Bologna) and ARSC (Fairbanks) supercomputing centers.

REFERENCES

Bruzual, G., & Charlot, S. 1993, ApJ, 405, 538
Carignan, C., Beaulieu, S., & Freeman, K. C. 1990, AJ, 99, 178
Colpi, M., Mayer, L., & Governato, F. 1999, ApJ, 525, 720
Cote, S., Freeman, K. C., & Carignan, C. 1997, in ASP Conf. Ser. 117, Dark and Visible Matter in Galaxies, ed. M. Persic & P. Salucci (San Francisco: ASP), 52
de Blok, W. J. G., & McGaugh, S. S. 1997, MNRAS, 290, 533
Dekel, A., & Silk, J. 1986, ApJ, 303, 39
Dikaiakos, M., & Stadel, J. 1996, Proc. Int. Conf. on Supercomputing (New York: Assoc. for Computing Machinery)
Einasto, J., Saar, E., Kaasik, A., & Chernin, A. D. 1974, Nature, 252, 111
Faber, S. M., & Lin, D. N. C. 1983, ApJ, 266, L17
Ferguson, H. C., & Binggeli, B. 1994, A&A Rev., 6, 67 (FB94)
Ghigna, S., Moore, B., Governato, F., Lake, G., Quinn, T., & Stadel, J. 1998, MNRAS, 300, 146
Grebel, E. K. 1999, in IAU Symp. 192, The Stellar Content of Local Group Galaxies, ed. P. Whitelock & R. Cannon (San Francisco: ASP), 17 (Gr99)
Guzmán, R., et al. 1997, ApJ, 489, 559
Hernandez, X., Gilmore, G., & Valls-Gabaud, D. 2000, MNRAS, 317, 831
Hernquist, L. 1993, ApJS, 86, 389
Hoffman, G. L., Salpeter, E. E., Farhat, B., Roos, T., Williams, H., & Helou, G. 1996, ApJS, 105, 269
Irwin, M., & Hatzdimitriou, D. 1995, MNRAS, 277, 1354
Jobin, M., & Carignan, C. 1990, AJ, 100, 648
Kennicutt, R. C., Jr. 1998, ApJ, 498, 541
Klypin, A., Kravtsov, A. V., Valenzuela, O., & Prada, F. 1999, ApJ, 522, 82
Lacey, C., & Cole, S. 1993, MNRAS, 262, 627
Lake, G. 1990, MNRAS, 244, 701
Little, B., & Tremaine, S. 1987, ApJ, 320, 493
Majewski, S. R., Ostheimer, J. C., Patterson, R. J., Kunkel, W. E., Johnston, K. V., & Geisler, D. 2000, AJ, 119, 760
Mateo, M. 1998, ARA&A, 36, 435 (Ma98)
Mo, H. J., Mao, S., & White, S. D. M. 1998, MNRAS, 296, 847
Moore, B., Ghigna, S., Governato, F., Lake, G., Quinn, T., Stadel, J., & Tozzi, P. 1999, ApJ, 524, L19

Moore, B., Katz, N., Lake, G., Dressler, A., & Oemler, A., Jr. 1996, Nature, 379, 613
Moore, B., Lake, G., & Katz, N. 1998, ApJ, 495, 139
Murali, C. 2000, ApJ, 529, L81
Peebles, P. J. E., Melott, A. L., Holmes, M. R., & Jiang, L. R. 1989, ApJ, 345, 108
Raha, N., Sellwood, J. A., James, R. A., & Kahn, F. D. 1991, Nature, 352, 411
van den Bergh, S. 1996, PASP, 108, 986
———. 1999, A&A Rev., 9, 273
Wilkinson, M. I., & Evans, N. W. 1999, MNRAS, 310, 645
Zwaan, M. A., van der Hulst, J. M., de Blok, W. J. G., & McGaugh, S. S. 1995, MNRAS, 273, L35